JAIST Repository
https://dspace.jaist.ac.jp/

Title	Imidazolium - Functionalized Fluorene - Based Anion Exchange Membrane (AEM) for Fuel Cell Applications
Author(s)	Salma, Umme; Zhang, Dishen; Nagao, Yuki
Citation	Wiley ChemistrySelect, 5(4): 1255-1263
Issue Date	2020-01-24
Type	Journal Article
Text version	author
URL	http://hdl.handle.net/10119/17076
Rights	This is the peer reviewed version of the following article: Copyright (C) 2020 Wiley-VCH. Umme Salma, Dishen Zhang, Yuki Nagao, Wiley ChemistrySelect, 5(4), 2020, pp.1255-1263, which has been published in final form at https://doi.org/10.1002/slct.201903246. This article may be used for non-commercial purposes in accordance with Wiley Terms and Conditions for Use of Self-Archived Versions.
Description	

JAIST
JAPAN
ADVANCED INSTITUTE OF
SCIENCE AND TECHNOLOGY

Japan Advanced Institute of Science and Technology

Imidazolium-Functionalized Fluorene-Based Anion Exchange Membrane (AEM) for Fuel Cell Applications

Umme Salma[a,b], Dishen Zhang[a], Yuki Nagao*[a]

[a] *School of Materials Science, Japan Advanced Institute of Science and Technology, 1-1 Asahidai, Nomi, Ishikawa 923-1292, Japan*

[b] *Department of Chemistry, Mawlana Bhashani Science and Technology University, Santosh, Tangail 1902, Bangladesh*

ABSTRACT

After a fluorene-based anion exchange membrane (AEM) containing 1-isopropyl-2-methylimidazolium with alkyl side chains was prepared, the membrane properties, including OH^- conductivities, ion exchange capacity (IEC), water uptake, swelling ratio, and chemical and thermal stabilities of the obtained membrane were assessed. The synthesized membrane exhibited low water uptake and good dimensional stability with adequate hydroxide conductivity. For example, the AEM showed a swelling ratio of 7% and hydroxide conductivity of 46 mS cm^{-1} at 80°C in liquid water. The chemical stability was investigated in 1 M NaOH solution at room temperature and at 80°C. At both temperatures, degradation of the imidazolium cationic groups was observed, although the main chain was chemically stable. All results obtained from this research are expected to provide important direction and insight for AEM synthesis for practical applications in anion exchange membrane fuel cells.

Introduction

Currently, polymer electrolyte membrane based fuel cells are emerging as a promising power source because of their high energy efficiency and low level of environmental pollution.[1] Anion exchange membrane fuel cells (AEMFCs) offer numerous advantages over traditional proton exchange membrane fuel cells (PEMFCs), such as faster kinetics of oxygen–reduction reaction, fuel flexibility, and reduced fuel crossover from anode to cathode. Several alternatives have been reported for using non-noble metal electrocatalysts: nickel, silver, and cobalt.[2]

For AEMFC development, a major challenge is finding a durable AEM that is adequately alkaline stable for long-term operation, and which has low water swelling and robust mechanical stability, while providing high ionic conductivity.[3] Aromatic polymers are desirable for researchers as a backbone of AEMs because they have high

chemical and thermal stability.[4] Many polymeric AEMs based on different backbones including polyether sulfones,[5] polyphenylenes,[6] polyphenylene oxides (PPO),[7] polystyrenes (PS),[8] polyarylene ether ketones (PAEK),[9] and polyolefins[10] have been studied extensively as AEM materials. Among the synthesized AEMs, polymer backbones containing electron-withdrawing groups with aryl ketone, aryl sulfone, and aryl ether bonds are vulnerable to nucleophilic attack by OH^- ions. Therefore, highly alkaline environment decrease chemical stability because of backbone degradation.[11]

Several cationic groups including quaternary ammonium (QA),[12] phosphonium,[13] sulfonium,[14] guanidinium,[15] imidazolium,[8, 16] benzimidazolium,[17] piperidinium, and morpholinium[18] have been used widely to synthesize polymeric membranes for AEMFCs. Among the different functional groups, tetraalkyl quaternary ammonium salts are most commonly used as cationic groups because of their easy synthesis procedures and inexpensive starting materials. Most AEMs are prepared by the addition of chloromethyl groups to the backbone of the polymer. Then QA salts are synthesized via quaternization reaction. However, the carcinogenic reagent chloromethyl methyl ether is very harmful to human health.[19] Another important difficulty is the efficient degradation of QA cations by several pathways that include Hofmann (β-hydrogen) or E2 elimination, ylide formation, and nucleophilic substitution (S_N2).[20] The ion exchange capacity (IEC) and ionic conductivity of AEMs decreases rapidly because of QA group degradation.

Mainly, AEMs containing imidazolium groups were found to have enhanced chemical stability in a highly alkaline environment with comparable ionic conductivity.[21] Researchers presumed that a π-conjugated structure is formed in heterocyclic imidazolium salts.[16, 22] The positive charges are delocalizing in the π-conjugated system. Also, nucleophilic attack via hydroxyl ions is hindered. However, imidazolium cations can degrade through a ring-opening reaction as the nucleophilic attack of OH^- ions[23] occurs at the C2 position, as shown in Scheme 1. Therefore, C2-substituted imidazolium cations are more stable in a highly alkaline condition. As an example, Yan *et al.*[16] reported that C2-substituted (methyl, isopropyl or phenyl group) imidazolium salts were more stable than a C2-unsubstituted one. This group also compared the chemical stability of some N3-substituted imidazolium and QA cations. The chemical stability was found from the LUMO energy, which was simulated using density functional theory (DFT). Among them, the imidazolium cation substituted by the isopropyl group showed the highest LUMO energy, which makes it the most stable imidazolium salt. They also confirmed the chemical stability of the imidazolium salts experimentally using model compounds.[24] As reported for another study, they used DFT calculations to investigate C2 substitution effects on LUMO energy by electron-

withdrawing and electron-donating groups. In their research, the amino-substituted imidazolium group showed the highest LUMO energy and alkaline stability. Cycloalkyl substitution at the N3 position can also markedly increase the LUMO energy. They observed that the LUMO energy of cycloheptyl-substituted and cyclooctyl-substituted imidazolium salt is higher than that of isopropyl-substituted imidazolium salt.[25] Therefore, they proposed that amino and cyclooctyl are the most suitable substituents for C2 and N3 substitution of imidazolium group. Coates *et al.* reported that the chemical stability of imidazolium salts was also improved dramatically by C4 and C5 substitution.[26] Fan *et al.* reported sterically protected poly(arylimidazolium) hydroxide exchange polymers that exhibited exceptional stability in 10 M KOH at high temperatures.[27]

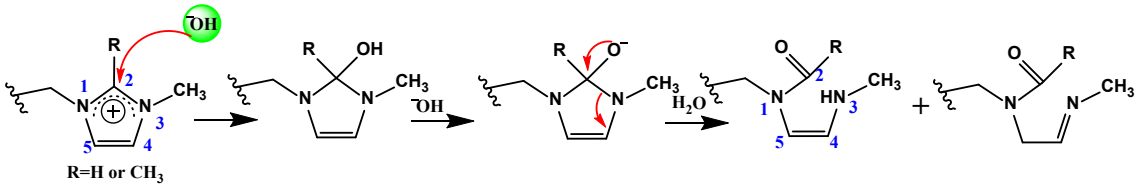

Scheme 1. Degradation mechanism of imidazolium cationic group.[23c]

Some researchers have observed high chemical stability of imidazolium cationic groups.[21, 28] Others have reported lower chemical stability of imidazolium cations.[6a, 18, 29] Despite high LUMO energies, imidazolium groups degraded in alkaline conditions. According to Yamaguchi *et al.*, the LUMO orbital of the imidazolium group is π-type; the HOMO orbital of OH^- ion is also π-type.[30] The interaction and overlapping between π–π orbitals of imidazolium and OH^- ion are greater than those of σ–π orbitals. Consequently, the imidazolium cationic groups with high LUMO energies degrade quickly in a basic condition. However, according to Marino and Kreuer, imidazolium cationic groups are unstable in basic conditions, even in mild conditions, because of the lack of steric shielding, because imidazolium groups are restricted to planar geometries.[31] In addition, the extended π-system increased the radical stabilization and the acidity of adjacent protons. To contribute this discrepancy state, we also synthesized imidazolium as a cationic group and incorporated it onto a polymer backbone. The synthesis procedure for 1-isopropyl-2-methylimidazole is simpler than that for the imidazoles described above. Therefore, we have chosen it as a cationic group.

Among the prepared AEMs, fluorenyl groups containing polymer backbones are garnering great attention because diverse chemical modifications are possible.[32] The molecular weights and the solubility of polymers can be enhanced by adding long alkyl or dialkyl groups at the C9-position of the fluorene ring. AEMs containing fluorene

groups on their backbone were found to have good thermal and alkaline stability aside from enhanced OH^- conductivity.[6b] Conjugated polymers based on fluorene groups also show good film-forming behavior.[33] The rigid and bulky fluorene groups on the backbone can form large interchain separations or free volumes by forcing each polymer chain apart. In the free volumes, water molecules might be confined.[34] Researchers observed that, in a high pH environment, the long alkyl tethered cationic groups show more thermal stability than the benzyl-substituted groups. Developed microphase separation and wider ion migration channels are observed in polymers containing a flexible side chain because a long side chain tends to form stronger self-assembly and hence wider ionic clusters.[35]

Because membranes are a fundamentally important component of fuel cells, strategies to synthesize high-performance AEMs are still being developed. The reduced thermochemical stability of AEMs hindered the practical use of AEMs in alkaline fuel cells. Many research groups have exerted great efforts to resolve these difficulties. For example, introducing long alkyl groups between cationic groups and polymer backbones,[36] forming different morphologies of polymers including graft,[37] block,[38] comb-shaped[39] or cluster-type[34] architectures, and using high concentrations of functional groups introduced to polymers by crosslinking[40] have been suggested as methods to enhance alkaline stability and hydroxide conductivity of AEMs.

The ion exchange capacity (IEC) value can increase by introducing more cationic groups and thereby increasing ion conductivity. Even though the high IEC enhances conductivity, the mechanical behavior of the resultant AEMs is affected very badly. Most synthesized AEMs with high IECs display chemical and physical instability. Because of high IECs, these membranes are unstable under fuel cell operating conditions (i.e., at 80°C, and high alkaline medium).[41] Consequently, researchers are strongly motivated to develop the chemical stability of polymer backbones and functional groups.

To determine the synthetic strategy, we have summarized the hydroxide conductivity, water uptake and ion exchange capacity of some reported AEMs based on different polymer backbone architectures presented in Table 1. We have also compared the alkaline stability of the membranes, although they were difficult to compare because researchers used different alkaline conditions and various techniques for stability tests. Our literature survey revealed that many research groups have used poly(arylene ether sulfone)s (PAES) and poly(phenylene oxide)s (PPO) as polymeric materials for AEM synthesis. However, a few of AEMs are available based on polyfluorenes.

Table 1. Comparison of hydroxide conductivity, water uptake, ion exchange capacity and alkaline stability of some state-of-the-art AEMs:

Membrane [Ref.]	Backbone type	IEC_{exp} (mmol g^{-1})	WU (%)	σ_{OH^-} (mS cm^{-1})	Alkaline Stability (1 M NaOH, 80°C)	Configuration
AI-PES-12 [39]	poly (arylene ether sulfone)	1.02	11.5	[a]140	13 days (2 M NaOH, 60°C) [c](no degradation)	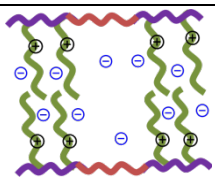
AI-PES-16 [39]		0.92	11.2	[a]120		
XE-Imd60 [40a]	poly (arylene ether sulfone)	2.43	92.4	[b]97	21 days (remaining conductivity 69%)	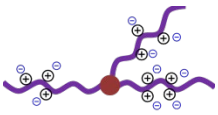
PPO-7Q-1.5 [36]	poly (phenylene oxide)	1.40	46.0	[a]64	8 days [d](no degradation)	
PPO-7Q-1.8 [36]		1.60	60.0	[a]85		
SIPN-60-2 [40b]	poly (phenylene oxide)	1.43	124.6	[a]68	30 days (remaining conductivity 74%)	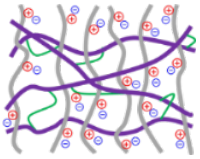
PPO5-4QPip-2.6 [42]	poly (phenylene oxide)	2.30	143.0	[a]221	10 days (1 M NaOH, 90°C) [d](no degradation)	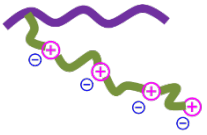
B-g-Q-1.5 [37]	poly (phenylene oxide)	1.55	66.5 (60°C)	[a]95	12 days (2 M NaOH, 60°C) (remaining IEC 63%)	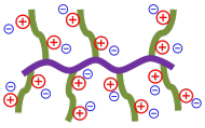
PFF^+ [6b]	poly (fluorene)s	2.45	26.0	[a]48	30 days [d](no degradation)	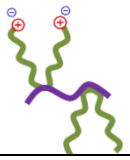

[a] in liquid water; [b] at relative humidity (100%); [c] from IEC and conductivity; [d] from ^{1}H NMR; ⊕, imidazolium; ⊕, quaternary ammonium; ⊕, piperidinium cationic groups.

Bae and coworkers[6b] reported that polyfluorene-based AEMs with long alkyl substituted QA groups were stable in 1 M NaOH at 80°C for 30 days. No report of the literature describes imidazolium-functionalized AEM with the same fluorene backbone. This research demonstrated a facile synthetic approach for an imidazolium-functionalized AEM with the same fluorene backbone and newly introduced 1-isopropyl-2-methylimidazolium as cationic groups by flexible alkyl side chains. The properties of the synthesized AEM, including the hydroxide conductivity, chemical and thermal stability, and water uptake and swelling ratio, were fully investigated.

Results and Discussion

Synthesis and Characterization of Monomers and Polymers

A facile synthetic procedure has been described as a result of this study for the synthesis of imidazolium functionalized fluorene-based AEM. The polyfluorene (PF) polymer synthesis strategy is shown in Scheme 2.

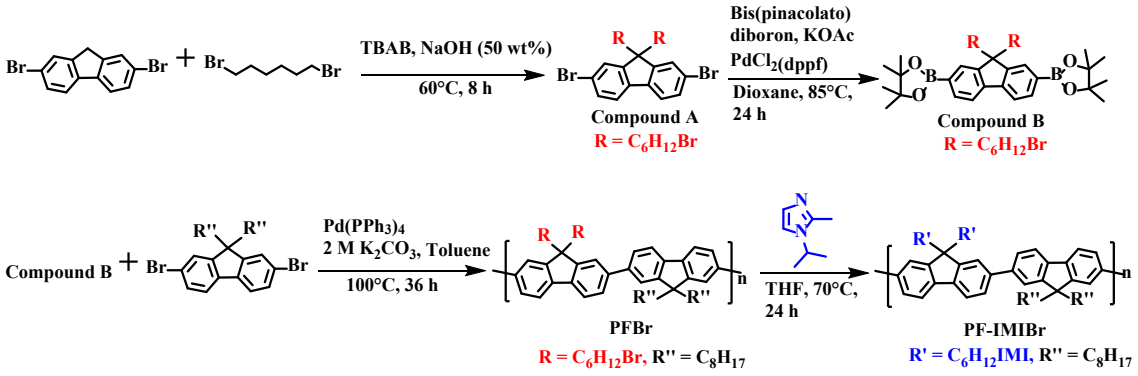

Scheme 2. Synthesis route of monomers and imidazolium functionalized fluorene-based polymer. Red stands for bromine-containing alkyl side chains. Blue shows imidazolium-containing alkyl side chains.

We have newly synthesized PF-IMIBr, a fluorene-based polymer, which has imidazolium groups on the long alkyl side chains. Detailed synthetic procedures are shown in the experimental section (see Supporting Information). The chemical structures of compounds A, B, and 1-isopropyl-2-methylimidazole were confirmed using ^{1}H NMR, ^{13}C NMR, and mass spectra (Supporting Information).

The chemical structure of the synthesized precursor PFBr was analyzed using ^{1}H NMR spectroscopy, as presented in Fig. 1A. The precursor PFBr polymer was soluble in tetrahydrofuran (THF) and chloroform. From GPC, the weight average molecular weight (Mw) of PFBr polymer was found to be 2.4×10^{4} (Table S1). The imidazolium group

containing Br^- form polyfluorene polymer PF-IMIBr was obtained using the reaction of PFBr and 1-isopropyl-2-methylimidazole (Scheme 2). The polyfluorene polymer (Br^- ion form) PF-IMIBr was soluble in organic solvents such as DMF, CH_3OH, and DMSO, but it was not soluble in H_2O.

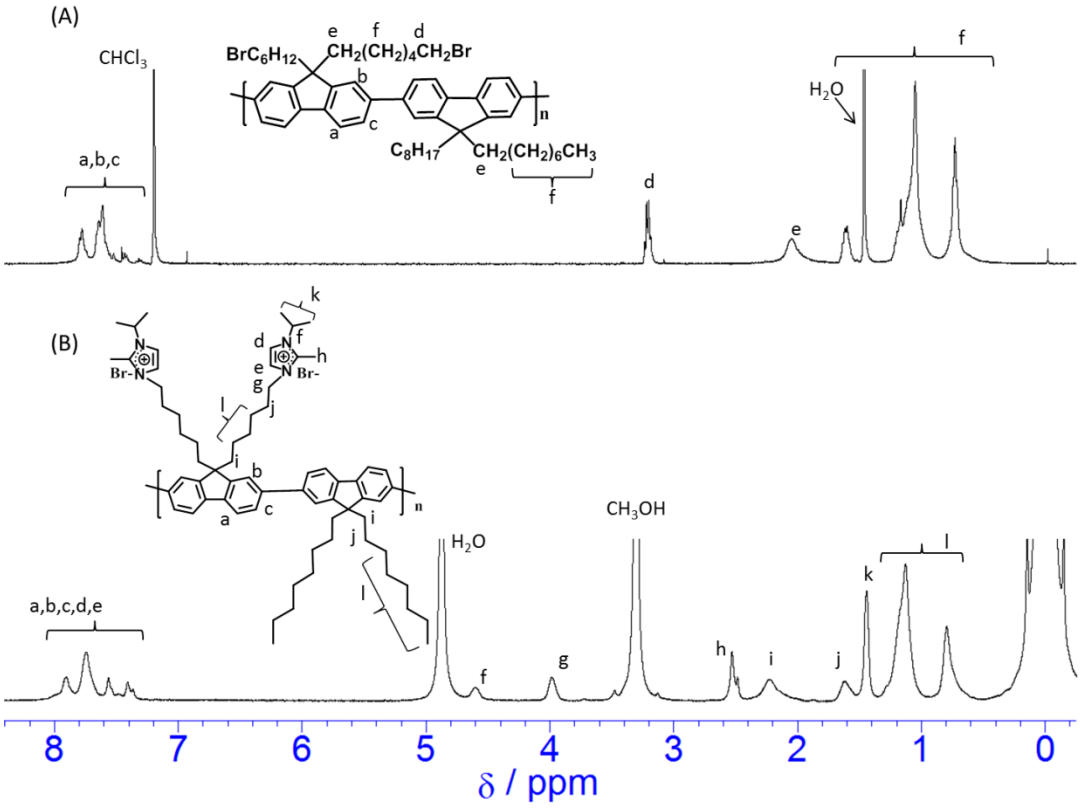

Fig. 1. ^1H NMR spectra of (A) PFBr and (B) PF-IMIBr.

Fig. 1B portrays the ^1H NMR spectrum of the synthesized Br^- form polymer: PF-IMIBr. New peaks at 7.55 ppm and 7.39 ppm are attributable to two aryl protons of the imidazolium group. Peaks at 4.6 ppm, 2.53 ppm, and 1.45 ppm are attributable to the isopropyl and methyl protons of the imidazolium cationic group. All new peaks indicate successful incorporation of imidazolium groups.

The chemical structure of copolymer was studied further using the FT-IR spectrum. The FT-IR spectra of the resultant polyfluorene copolymer PFBr and PF-IMIBr are presented in Fig. 2. The C–H absorption bands of both polymers for methylene ($-CH_2$) were observed respectively at 2853 and 2927 cm^{-1} for symmetric and asymmetric vibrations. The presence of polyphenylene was confirmed by absorption bands at 1603 and 1458 cm^{-1}. The peaks around 1578 cm^{-1} and 1522 cm^{-1} in PF-IMIBr polymer were attributed to the stretching vibration of C=N. Also, an absorption band at 1181 cm^{-1} was

observed for the C–N bond of imidazolium group. Results confirmed that the incorporation of imidazolium cation onto the polymer was successful. Furthermore, a strong and broad band at 3400 cm^{-1} was found for imidazolium-functionalized polymer. It was attributed to the stretching vibration of O–H bonds of water. The improved hydrophilic property of PF-IMIBr polymer also confirmed the successful attachment of imidazolium groups on the polymer.

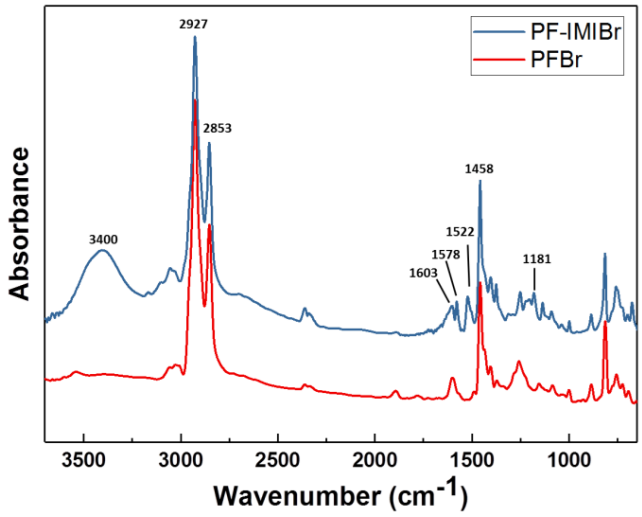

Fig. 2. FT-IR spectra of PFBr and PF-IMIBr.

The EDX spectra before and after ion exchange of Br^- form to OH^- form, as depicted in Fig. 3A to Fig. 3B, confirm that more than 91% Br^- ions were exchanged by OH^-. Zhuo *et al.*[43] also found that bromine elements of AEMs had decreased or had almost disappeared after alkalization using KOH aqueous solution from EDX spectra. The EDX spectra further confirmed the sufficient conversion of alkyl Br groups and successful alkalization.

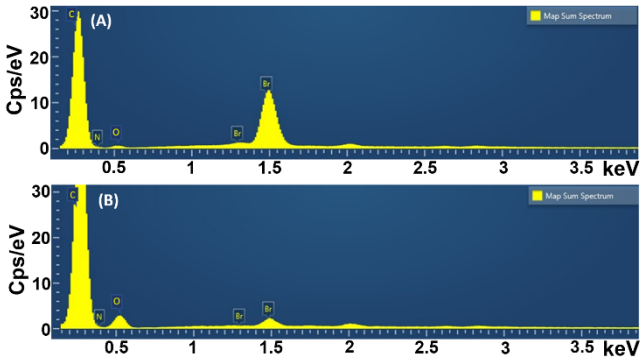

Fig. 3. EDX spectra for (A) PF-IMIBr and (B) PF-IMI membranes.

Membrane Morphology

Membranes were fabricated from 4 wt% solutions in DMF and were cast on a flat PTFE sheet. After removing the solvent, the resultant membranes become transparent, as portrayed in Fig. 4A. Using SEM, the PF-IMIBr membrane morphology was investigated. As shown in Figs. 4B and 4C, the SEM images revealed that the surface and cross-section of the resultant polymer membranes are uniform, tight and dense, with no pores visible at this scale.

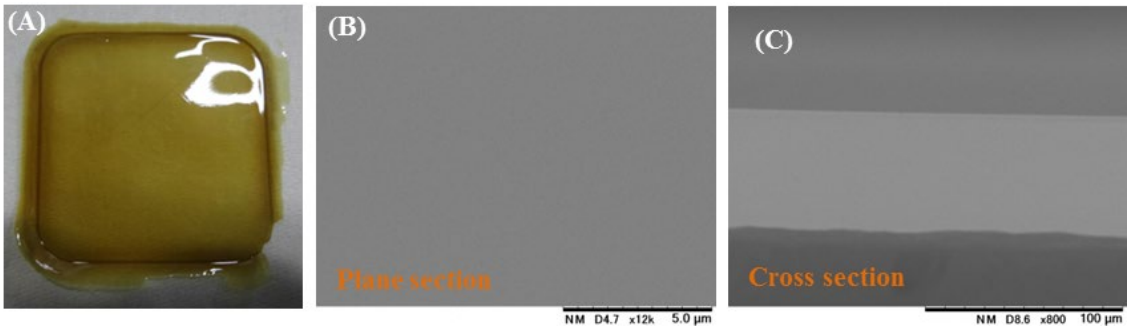

Fig. 4. (A) Photograph of the membrane and SEM images of the PF-IMIBr, (B) plane section, and (C) cross section of the polymer.

Thermal Stability

Thermal stability is a primary concern for AEMs because some AEMs containing benzyl quaternary ammonium cationic groups usually show instability of cationic groups at temperatures higher than 120°C.[44] Because aromatic polymers have outstanding thermal stability, aromatic backbones are the preferred candidates for application in high-temperature AEMFCs. Fig. 5 presents results of the thermogravimetric analysis. The first weight loss below 200°C has less than 4 wt%. This weight loss originates from evaporation of absorbed water in the membrane. The second loss between 220°C and 300°C is probably attributable to degradation of the imidazolium cations and the alkyl side chains of the polymer. The third degradation at temperatures higher than 390°C might be attributable to decomposition of the polyfluorene backbones. The thermal stability of long alkyl tethered imidazolium cationic groups in this study is much higher than that of the benzyl substituted quaternary ammonium groups. The result showed that the thermal stability of the synthesized AEM is comparable to the reported imidazolium containing AEM [28a] and long alkyl-tethered QA containing polyfluorene backbone.[6b]

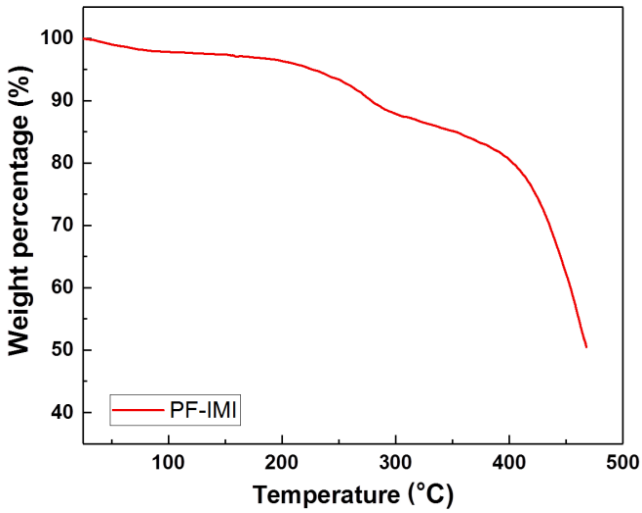

Fig. 5. TGA graph of PF-IMI under N_2 flow. Heating rate: 10°C min^{-1}.

The overall result of thermal analysis implies that the resultant polyfluorene polymer maintains high thermal stability up to 200°C, which is far beyond the desired temperature range for fuel cell applications. To elucidate the thermal behavior of OH^- containing polymer (PF-IMI), DSC was also tried, as shown in Fig. S7.

Water Uptake (WU), Swelling Ratio (SR), and Ion Exchange Capacity (IEC)

Water uptake plays an important role in ion conductivity. The membrane swelling behavior of is a critical factor that influences the morphologic stability and mechanical properties of membranes. Excessive WU might engender mechanical weakness and over-swelling. Commonly, the WU and swelling ratio also increases with increasing ion exchange capacity (IEC). The IEC of membranes is responsible for ion transfer and therefore influences the ion conductivity. The IEC of the synthesized membrane was measured using the back titration method. It was found to be 1.84 mmol/g. The experimental IEC shows good agreement with the calculated value of 1.99 mmol/g obtained from the chemical structure. Water uptake of the membranes increased from 19 to 32 wt% with increasing temperature from 20°C to 80°C (Fig. 6) because the mobility of the polymer molecules is enhanced and higher free volume results from the opening of the micropores at high temperatures. Consequently, hydrated ion clusters are formed, which engender increased water adsorption.[45] With increasing temperature from 20°C to 80°C, the swelling ratio of the synthesized membrane increased from 1% to 7%.

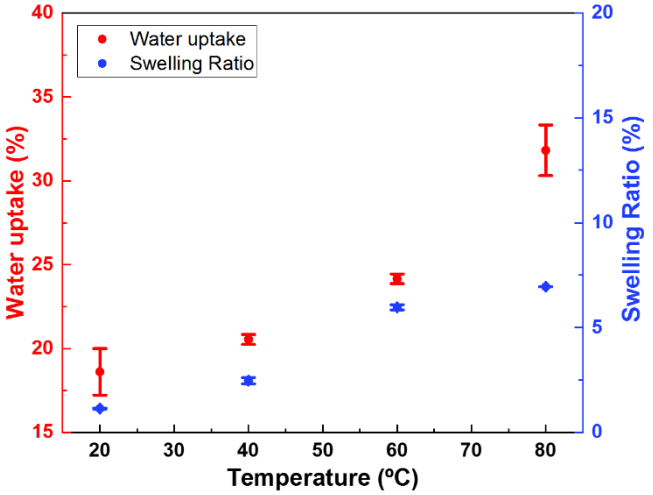

Fig. 6. Water uptake and swelling ratio of the PF-IMI membrane.

The water uptake and degrees of swelling of the resultant polymer are lower than those of other reported aromatic AEMs [e.g., polyarylene ether sulfones[46] and quaternized polyarylene ether ketones[47]] with similar IEC values. The absence of flexible groups (such as thioether and ether bonds) and the stiff aromatic backbone of the membrane can suppress the water uptake. In addition, the water uptake and swelling ratio of the synthesized AEM are comparable with the AEM (PFF^{+}) containing similar type of polyfluorene backbone.[6b] Therefore, the good dimensional stability of the membrane can be expected as a feasible approach for AEMFC application.

Hydroxide Ion Conductivity and Activation Energy

The OH^{-} ion conductivity of the polymeric membranes plays an important role in fuel cell performance. The polyfluorene polymeric membrane showed hydroxide conductivity of 7 mS cm^{-1} at 20°C and increased to 46 mS cm^{-1} at 80°C, as portrayed in Fig. 7. The conductivity of AEMs increases concomitantly with increasing temperature because of faster ionic migration and higher water molecule diffusion. Simultaneously, at

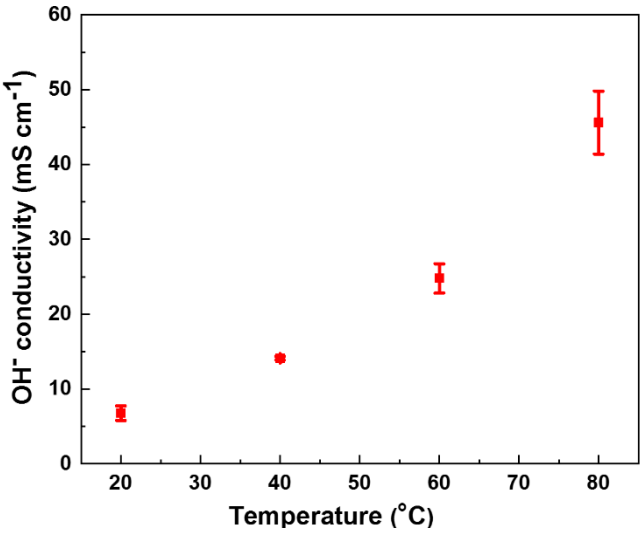

Fig. 7. Temperature dependence of the OH^- conductivity of PF-IMI polymer.

a higher temperature, the flexibility of the polymer chains increases and membranes adsorb more water, resulting in more water-swollen membranes and wider ion-conducting channels, leading to more enhanced ion transfer.[22, 48] The conductivity of the resultant AEM is comparable to the hydroxide conductivity of other membranes having similar IEC values.[49]

From the Arrhenius plot showing the conductivity–temperature relation, the activation energy (E_a) of the hydroxide conduction was determined from Fig. S8. The plot shows that the hydroxide conductivity of the polymer followed the Arrhenius behavior at temperatures of 20–80°C. The activation energy of polyfluorene polymer PF-IMI is 27 kJ mol^{-1}, which is comparable to those of some reported AEMs.[50] This activation energy reflects the more sterically hindered environment of the imidazolium hydroxide groups.

For better understanding of the performance of the polyfluorene polymer, the IEC, WU, and hydroxide conductivity are summarized with some reported imidazolium functionalized AEMs such as polyaryl ether ketones (MIPAEKs),[49] polyaryl ether sulfones,[51] polyaryl ethers,[52] PPO,[53] and cross linked[22, 50a] AEMs with similar IEC values, as shown in Table 2. The presence of water in AEMs is crucially important for hydroxide conductivity, but dimensional instability might result from excessive water uptake. Because of the rigid backbone of the polyfluorene polymer of this study and without flexible thioether or ether bonds, the water uptake is lower than for other AEMs described in Table 2. The hydroxide conductivity of the synthesized AEM is comparable to that of the reported AEMs, but less than ImPES-0.45 and trimPES-0.4 with multi-imidazolium. Furthermore, the hydroxide conductivities of PP-60, $[PVMIm][OH]_{40}$-DVB_4 and ANM-22-100 AEMs are markedly higher than those of PF-IMI because of

their high water uptake.

Table 2. Comparison of IEC, WU, and hydroxide conductivity of PF-IMI with some representative AEMs at 80°C

Membrane	IEC (mmol g^{-1})		WU (wt%)	σ_{OH^-}
	Cal.[a]	Exp.[b]		(mS cm^{-1})
PF-IMI	1.99	1.84 ± 0.03	32.0	46
MIPAEK-b[49a]		1.97	70.5	35
MIPAEK-c[49a]		2.57	84.0	39
MIPAEK-SF-c[49a]		1.81	73.7	30
MIPAEK-SF-d[49a]		1.89	82.8	33
CL-8C/PAEK/UnIm0.2MeIm0.8[49b]	2.82	1.91	51.7	40
PP-60[50a]	2.63	1.98	36.6 (60°C)	60
C-FPAEO-75-MIM[52]		1.80	76.0 (60°C)	36
ImPES-0.45[51a]	1.95	1.84	57.3 (60°C)	112
trimPES-0.4[51b]	2.34	2.03	62.0 (60°C)	120
[PVMIm][OH]$_{40}$-DVB$_4$[22]	1.60	1.47	157.0[c]	53.5 (60°C)
[PUVBIm][OH][51c]	1.80	1.65		40
PSf-ImmOH-70[51d]	2.06	1.94	129.0 (60°C)	26 (60°C)
ANM-22-100[53]	1.82	1.67	22.0 (30°C)	78 (60°C)

[a] calculated from chemical structure; [b] value obtained using titration experimentation; [c] room temperature

Alkaline Stability

A major challenge of AEMs for practical application is thermochemical stability, particularly in high-temperature operations of alkaline fuel cells. The OH^- form membranes were soaked in a 1 M NaOH solution at 80°C for 168 h and 360 h to assess the chemical stability. Changes in the chemical structures of AEMs were investigated using FT-IR spectra. We have tried to analyze the degradation of polymer membranes using the ^{1}H NMR spectrum. Unfortunately, the OH^- containing polymers were not soluble in ^{1}H NMR solvents such as DMSO, CH_3OH, H_2O, and $CHCl_3$. The tested membranes retained the membrane shape. No visible changes were found after alkaline treatment. Fig. 8 shows the time dependence of the FT-IR spectra of PF-IMI (OH^- form) membrane by alkaline treatment at 80°C. After the alkaline test, the absorbance of the

conjugated C=N band at 1576 and 1518 cm^{-1} decreased considerably with the treatment time, which indicates that imidazolium cations were degraded by the attack of OH^- at the C2 position of the imidazolium ring, as shown in Scheme 3.[23c] By the addition of OH^- on the imidazolium ring, a nonaromatic intermediate structure is generated. Because this produced transition state structure is unstable. An aldehyde/keto group containing product is formed irreversibly. It stimulates the decomposition of imidazolium-containing AEMs[54]. Ye *et al.*[55] observed an aldehyde group in their ^1H NMR results attributable to the degradation of imidazolium cation. The possible mechanism of degradation for the imidazolium group is presented in Scheme 3.

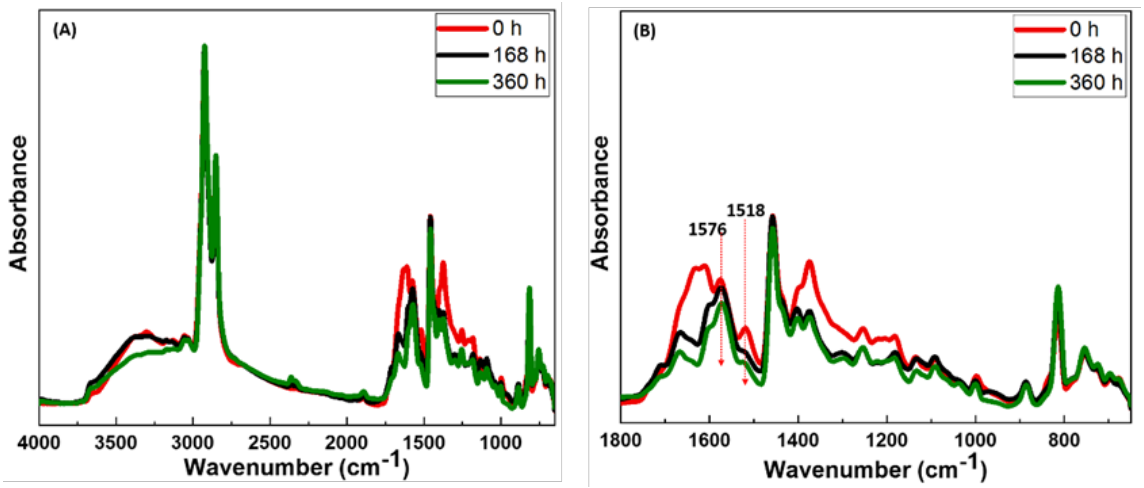

Fig. 8. (A) FT-IR spectra of PF-IMI (OH^- form) membrane and OH^- form after alkaline stability test. (B) Close-up image of the region of 1800–650 cm^{-1}, showing changes in peak intensity.

The absorption band of O–H stretching vibrations of water at 3400 cm^{-1} decreased after alkaline treatment. This decrease might be related to the decrease of hydrophilic imidazolium cationic groups. As we have observed the degradation of imidazolium groups at 80°C, we also investigated degradation at room temperature. Moreover, surprisingly, we found that imidazolium cationic groups also degraded at room temperature (see Supporting Information).

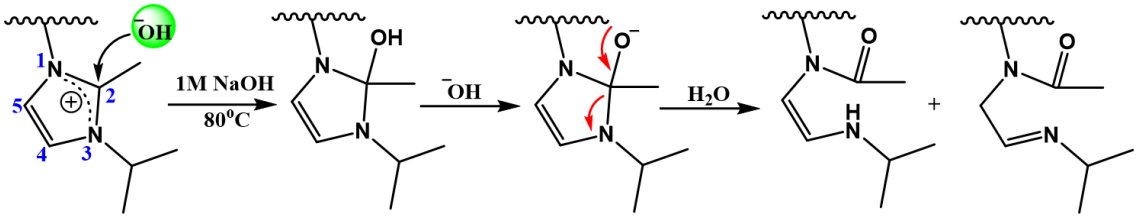

Scheme 3. Possible degradation mechanism of 1-isopropyl-2-methylimidazolium cation in a high alkaline condition.

Although some reports of the literature[21, 28] have suggested high chemical stability of imidazolium cationic groups, other reports[6a, 18, 29] have revealed that the imidazolium cations are less stable in high alkaline conditions. We also observed the degradation of the imidazolium cationic group, even at room temperature. Based on work by Bae and co-workers,[6b] we conclude that alkyl-tethered imidazolium with isopropyl group is even less stable than alkyl-tethered quaternary ammonium groups in fluorene backbone. We conclude that 1-isopropyl-2-methylimidazolium cationic groups are not stable in fluorene backbone. Yan and coworkers reported 2-amino-1-methyl-3-cyclooctylimidazolium as a cationic group with the highest LUMO energy, which indicates its highest chemical stability among their investigated imidazolium cationic groups. Therefore, 2-amino-1-methyl-3-cyclooctylimidazolium is a candidate for an alkaline stable imidazolium cationic group in AEMs, which might offer potential advancement on fluorene structures.

Conclusions

In summary, an alkyl 1-isopropyl-2-methylimidazolium functionalized fluorene-based AEM was synthesized. Then its membrane properties were analyzed. The polyfluorene polymer was prepared using the Suzuki cross-coupling reaction and was cast from DMF solvent, followed by ion exchange with OH^- anions. The prepared membrane showed high thermal stability, high anion exchange capacity, a low swelling ratio, and moderate water uptake. The AEM membrane exhibited hydroxide conductivity of 46 mS cm^{-1} at 80°C. We investigated that the imidazolium cationic group degraded at 80°C even at room temperature in alkaline medium. From this study, we have contributed to the discussion of discrepancies reported in the literature for imidazolium alkaline stability. The chemical stability of imidazolium with isopropyl group was found to be less than that of quaternary ammonium groups in the fluorene backbone. This investigation will assist researchers in choosing cationic groups for synthesizing alkaline-stable AEMs for actual application in AEMFCs.

Supporting Information Summary

Supporting information includes materials, synthesis procedures for monomers and polymers, characterizations and measurements including ^{1}H and ^{13}C NMR spectroscopy, Fourier-transform infrared (FT-IR) spectroscopy, mass spectroscopy, gel permeation chromatography (GPC), energy dispersive X-ray spectroscopy (EDX), scanning electron microscopy (SEM), thermogravimetric analysis (TGA), differential scanning calorimetry (DSC), water uptake, swelling ratio, ion exchange capacity (IEC), hydroxide ion conductivity, and alkaline stability at room temperature. GPC results of precursor PFBr polymer.

Acknowledgments

We thank Professor Noriyoshi Matsumi of the Japan Advanced Institute of Science and Technology (JAIST) for providing a glovebox. We are also grateful to Professor Kazuaki Matsumura at JAIST for supporting DSC measurements. We sincerely express our appreciation to Associate professor Shusaku Nagano at Nagoya University for GPC measurement. We gratefully appreciate the support of Dr. Akio Miyazato (technical staff of mass spectrometry, JAIST) for mass spectrum measurements. We also gratefully acknowledge Associate Professor Guangtong Wang (Harbin Institute of Technology, China) for his cordial assistance during polymer synthesis.

Conflict of Interest

The authors have no conflict of interest to declare.

Author information

Corresponding author

Dr. Yuki Nagao

E-mail: ynagao@jaist.ac.jp Phone: +81(Japan)-761-51-1541, Fax: +81(Japan)-761-51-1149 Address: 1-1 Asahidai, Nomi, Ishikawa 923-1292, Japan.

Funding

This work was partially supported by JSPS KAKENHI Grant Number JP18K05257.

Keywords: 1-isopropyl-2-methylimidazole · alkaline stability · anion exchange membrane · flexible alkyl side chains · polyfluorene

References

[1] a) K. H. Gopi, S. G. Peera, S. Bhat, P. Sridhar, S. Pitchumani, *Int. J. Hydrogen Energy* **2014**, *39*, 2659–2668; b) W. Lu, Z.-G. Shao, G. Zhang, Y. Zhao, J. Li, B. Yi, *Int. J. Hydrogen Energy* **2013**, *38*, 9285–9296.

[2] a) M. A. Hickner, A. M. Herring, E. B. Coughlin, *J. Polym. Sci., Part B: Polym. Phys.* **2013**, *51*, 1727–1735; b) H. Zhang, P. K. Shen, *Chem. Rev.* **2012**, *112*, 2780–2832; c) D. R. Dekel, *J. Power Sources* **2018**, *375*, 158–169; d) S. Lu, J. Pan, A. Huang, L. Zhuang, J. Lu, *Proc. Natl. Acad. Sci.* **2008**, *105*, 20611–20614.

[3] a) S. A. Nuñez, M. A. Hickner, *ACS Macro Lett.* **2012**, *2*, 49–52; b) Q. Zhang, S. Li, S. Zhang, *Chem. Commun.* **2010**, *46*, 7495–7497.

[4] P. Y. Xu, K. Zhou, G. L. Han, Q. G. Zhang, A. M. Zhu, Q. L. Liu, *ACS Appl. Mater. Interfaces* **2014**, *6*, 6776–6785.

[5] a) N. Li, Q. Zhang, C. Wang, Y. M. Lee, M. D. Guiver, *Macromolecules* **2012**, *45*, 2411–2419; b) Z. Zhao, J. Wang, S. Li, S. Zhang, *J. Power Sources* **2011**, *196*, 4445–4450.

[6] a) M. R. Hibbs, *J. Polym. Sci., Part B: Polym. Phys.* **2013**, *51*, 1736–1742; b) W.-H. Lee, A. D. Mohanty, C. Bae, *ACS Macro Lett.* **2015**, *4*, 453–457.

[7] a) H.-S. Dang, P. Jannasch, *Macromolecules* **2015**, *48*, 5742–5751; b) S. He, L. Liu, X. Wang, S. Zhang, M. D. Guiver, N. Li, *J. Membr. Sci.* **2016**, *509*, 48–56.

[8] X. Ren, S. C. Price, A. C. Jackson, N. Pomerantz, F. L. Beyer, *ACS Appl. Mater. Interfaces* **2014**, *6*, 13330–13333.

[9] W. Ma, C. Zhao, H. Lin, G. Zhang, H. Na, *J. Appl. Polym. Sci.* **2011**, *120*, 3477–3483.

[10] a) A. N. Lai, K. Zhou, Y. Z. Zhuo, Q. G. Zhang, A. M. Zhu, M. L. Ye, Q. L. Liu, *J. Membr. Sci.* **2016**, *497*, 99–107; b) M. Zhang, C. Shan, L. Liu, J. Liao, Q. Chen, M. Zhu, Y. Wang, L. An, N. Li, *ACS Appl. Mater. Interfaces* **2016**, *8*, 23321–23330.

[11] a) A. D. Mohanty, S. E. Tignor, J. A. Krause, Y.-K. Choe, C. Bae, *Macromolecules* **2016**, *49*, 3361–3372; b) J. S. Olsson, T. H. Pham, P. Jannasch, *Macromolecules* **2017**, *50*, 2784–2793; c) E. J. Park, Y. S. Kim, *J. Mater. Chem. A* **2018**, *6*, 15456–15477.

[12] H.-S. Dang, P. Jannasch, *J. Mater. Chem. A* **2017**, *5*, 21965–21978.

[13] K. J. Noonan, K. M. Hugar, H. A. Kostalik IV, E. B. Lobkovsky, H. D. Abruña, G. W. Coates, *J. Am. Chem. Soc.* **2012**, *134*, 18161–18164.

[14] B. Zhang, S. Gu, J. Wang, Y. Liu, A. M. Herring, Y. Yan, *RSC Adv.* **2012**, *2*, 12683–12685.

[15] X. Lin, L. Wu, Y. Liu, A. L. Ong, S. D. Poynton, J. R. Varcoe, T. Xu, *J. Power*

Sources **2012**, *217*, 373–380.

[16] B. Lin, H. Dong, Y. Li, Z. Si, F. Gu, F. Yan, *Chem. Mater.* **2013**, *25*, 1858–1867.

[17] a) O. D. Thomas, K. J. Soo, T. J. Peckham, M. P. Kulkarni, S. Holdcroft, *J. Am. Chem. Soc.* **2012**, *134*, 10753–10756; b) A. G. Wright, J. Fan, B. Britton, T. Weissbach, H.-F. Lee, E. A. Kitching, T. J. Peckham, S. Holdcroft, *Energy Environ. Sci.* **2016**, *9*, 2130–2142.

[18] H. Lim, B. Lee, D. Yun, A. Z. Al Munsur, J. E. Chae, S. Y. Lee, H.-J. Kim, S. Y. Nam, C. H. Park, T.-H. Kim, *ACS Appl. Mater. Interfaces* **2018**, *10*, 41279–41292.

[19] M. Zhang, H. K. Kim, E. Chalkova, F. Mark, S. N. Lvov, T. M. Chung, *Macromolecules* **2011**, *44*, 5937–5946.

[20] a) S. Chempath, J. M. Boncella, L. R. Pratt, N. Henson, B. S. Pivovar, *J. Phys. Chem. C* **2010**, *114*, 11977–11983; b) S. Chempath, B. R. Einsla, L. R. Pratt, C. S. Macomber, J. M. Boncella, J. A. Rau, B. S. Pivovar, *J. Phys. Chem. C* **2008**, *112*, 3179–3182.

[21] B. Qiu, B. Lin, L. Qiu, F. Yan, *J. Mater. Chem.* **2012**, *22*, 1040–1045.

[22] B. Lin, L. Qiu, J. Lu, F. Yan, *Chem. Mater.* **2010**, *22*, 6718–6725.

[23] a) X. Lin, J. R. Varcoe, S. D. Poynton, X. Liang, A. L. Ong, J. Ran, Y. Li, T. Xu, *J. Mater. Chem. A* **2013**, *1*, 7262–7269; b) Z. Si, L. Qiu, H. Dong, F. Gu, Y. Li, F. Yan, *ACS Appl. Mater. Interfaces* **2014**, *6*, 4346–4355; c) S. Gottesfeld, D. R. Dekel, M. Page, C. Bae, Y. Yan, P. Zelenay, Y. S. Kim, *J. Power Sources* **2018**, *375*, 170–184.

[24] F. Gu, H. Dong, Y. Li, Z. Si, F. Yan, *Macromolecules* **2013**, *47*, 208–216.

[25] H. Dong, F. Gu, M. Li, B. Lin, Z. Si, T. Hou, F. Yan, S. T. Lee, Y. Li, *ChemPhysChem* **2014**, *15*, 3006–3014.

[26] K. M. Hugar, H. A. Kostalik IV, G. W. Coates, *J. Am. Chem. Soc.* **2015**, *137*, 8730–8737.

[27] a) J. Fan, S. Willdorf-Cohen, E. M. Schibli, Z. Paula, W. Li, T. J. Skalski, A. T. Sergeenko, A. Hohenadel, B. J. Frisken, E. Magliocca, *Nat. Commun.* **2019**, *10*, 2306; b) J. Fan, A. G. Wright, B. Britton, T. Weissbach, T. J. Skalski, J. Ward, T. J. Peckham, S. Holdcroft, *ACS Macro Lett.* **2017**, *6*, 1089–1093.

[28] a) B. Lin, L. Qiu, B. Qiu, Y. Peng, F. Yan, *Macromolecules* **2011**, *44*, 9642–9649; b) W. Li, J. Fang, M. Lv, C. Chen, X. Chi, Y. Yang, Y. Zhang, *J. Mater. Chem.* **2011**, *21*, 11340–11346; c) Z. Sun, B. Lin, F. Yan, *ChemSusChem* **2018**, *11*, 58–70.

[29] O. I. Deavin, S. Murphy, A. L. Ong, S. D. Poynton, R. Zeng, H. Herman, J. R. Varcoe, *Energy Environ. Sci.* **2012**, *5*, 8584–8597.

[30] K. Matsuyama, H. Ohashi, S. Miyanishi, H. Ushiyama, T. Yamaguchi, *RSC Adv.* **2016**, *6*, 36269–36272.

[31] M. Marino, K. Kreuer, *ChemSusChem* **2015**, *8*, 513–523.

[32] a) D. Chen, M. A. Hickner, S. Wang, J. Pan, M. Xiao, Y. Meng, *Int. J. Hydrogen Energy* **2012**, *37*, 16168–16176; b) P. Y. Xu, K. Zhou, G. L. Han, Q. G. Zhang, A. M. Zhu, Q. L. Liu, *J. Membr. Sci.* **2014**, *457*, 29–38.

[33] K. Lee, H. J. Kim, J. Kim, *Adv. Funct. Mater.* **2012**, *22*, 1076–1086.

[34] M. Tanaka, K. Fukasawa, E. Nishino, S. Yamaguchi, K. Yamada, H. Tanaka, B. Bae, K. Miyatake, M. Watanabe, *J. Am. Chem. Soc.* **2011**, *133*, 10646–10654.

[35] C. Wang, N. Li, D. W. Shin, S. Y. Lee, N. R. Kang, Y. M. Lee, M. D. Guiver, *Macromolecules* **2011**, *44*, 7296–7306.

[36] H.-S. Dang, E. A. Weiber, P. Jannasch, *J. Mater. Chem. A* **2015**, *3*, 5280–5284.

[37] J. Ran, L. Wu, T. Xu, *Polym. Chem.* **2013**, *4*, 4612–4620.

[38] L. Wang, M. A. Hickner, *J. Mater. Chem. A* **2016**, *4*, 15437–15449.

[39] A. H. Rao, S. Nam, T.-H. Kim, *J. Mater. Chem. A* **2015**, *3*, 8571–8580.

[40] a) K. H. Lee, D. H. Cho, Y. M. Kim, S. J. Moon, J. G. Seong, D. W. Shin, J.-Y. Sohn, J. F. Kim, Y. M. Lee, *Energy Environ. Sci.* **2017**, *10*, 275–285; b) J. Pan, L. Zhu, J. Han, M. A. Hickner, *Chem. Mater.* **2015**, *27*, 6689–6698.

[41] C. E. Diesendruck, D. R. Dekel, *Curr. Opin. Electrochem.* **2018**, *9*, 173–178.

[42] H.-S. Dang, P. Jannasch, *ACS Appl. Energy Mater.* **2018**, *1*, 2222–2231.

[43] Y. Z. Zhuo, A. N. Lai, Q. G. Zhang, A. M. Zhu, M. L. Ye, Q. L. Liu, *J. Membr. Sci.* **2015**, *491*, 138–148.

[44] J. Pan, S. Lu, Y. Li, A. Huang, L. Zhuang, J. Lu, *Adv. Funct. Mater.* **2010**, *20*, 312–319.

[45] a) F. Bu, C. Zhao, B. Wang, N. Zhang, H. Lu, Z. Cai, Y. Zhang, H. Na, *RSC Adv.* **2015**, *5*, 57067–57075; b) G. Merle, M. Wessling, K. Nijmeijer, *J. Membr. Sci.* **2011**, *377*, 1–35.

[46] A. D. Mohanty, Y.-B. Lee, L. Zhu, M. A. Hickner, C. Bae, *Macromolecules* **2014**, *47*, 1973–1980.

[47] D. Chen, M. A. Hickner, *Macromolecules* **2013**, *46*, 9270–9278.

[48] F. Zhang, H. Zhang, C. Qu, *J. Mater. Chem.* **2011**, *21*, 12744–12752.

[49] a) Y. Song, C. Liu, J. Zhao, J. Luo, *Int. J. Hydrogen Energy* **2016**, *41*, 10446–10457; b) Y. Xu, J. Yang, N. Ye, M. Teng, R. He, *Eur. Polym. J.* **2015**, *73*, 116–126.

[50] a) D. Guo, Y. Z. Zhuo, A. N. Lai, Q. G. Zhang, A. M. Zhu, Q. L. Liu, *J. Membr. Sci.* **2016**, *518*, 295–304; b) X. Li, Q. Liu, Y. Yu, Y. Meng, *J. Mater. Chem. A* **2013**,

1, 4324–4335.

[51] a) D. Guo, A. N. Lai, C. X. Lin, Q. G. Zhang, A. M. Zhu, Q. L. Liu, *ACS Appl. Mater. Interfaces* **2016**, *8*, 25279–25288; b) D. Guo, C. X. Lin, E. N. Hu, L. Shi, F. Soyekwo, Q. G. Zhang, A. M. Zhu, Q. L. Liu, *J. Membr. Sci.* **2017**, *541*, 214–223; c) Z. Si, Z. Sun, F. Gu, L. Qiu, F. Yan, *J. Mater. Chem. A* **2014**, *2*, 4413–4421; d) Y. Yang, J. Wang, J. Zheng, S. Li, S. Zhang, *J. Membr. Sci.* **2014**, *467*, 48–55.

[52] W. Wang, S. Wang, W. Li, X. Xie, *Int. J. Hydrogen Energy* **2013**, *38*, 11045–11052.

[53] A. N. Mondal, Y. He, L. Wu, M. I. Khan, K. Emmanuel, M. M. Hossain, L. Ge, T. Xu, *J. Mater. Chem. A* **2017**, *5*, 1022–1027.

[54] K. M. Meek, Y. A. Elabd, *Macromolecules* **2015**, *48*, 7071–7084.

[55] Y. Ye, Y. A. Elabd, *Macromolecules* **2011**, *44*, 8494–8503.

Graphical Abstract
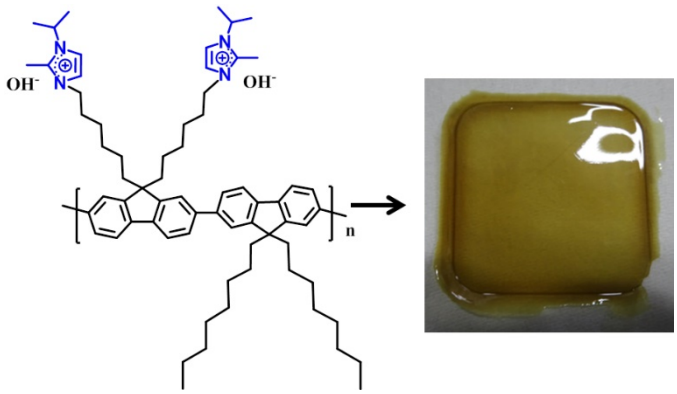
Polyfluorene polymer with alkyl imidazolium cationic groups was newly synthesized. Membranes exhibited high OH^- conductivity and good thermal stability. Lower water uptake suppressed dimensional expansion of the membrane. Imidazolium groups degraded in highly alkaline media but the fluorene backbone remained chemically stable. We discussed discrepancies presented in the relevant literature.